Earthquake Geotechnical Engineering for Protection and Development of Environment and Constructions – Silvestri & Moraci (Eds)
ISBN 978-0-367-14328-2

Repeated cyclic shear loading response of reconstituted Fraser River silt

A. Soysa & D. Wijewickreme
University of British Columbia, Canada

ABSTRACT: Assessing the dynamic response of soil in the laboratory often comprises conducting cyclic shear tests involving triaxial or direct simple shear test apparatus. In some cases, either post-cyclic monotonic shear loading or post-cyclic reconsolidation loading are performed to assess the liquefied-strength or post-seismic settlement characteristics, respectively. However, tests conducted with repeated cyclic loading phases applied on soil specimens reconsolidated after previous loadings is very limited. Repeated cyclic loading can provide insight with respect to the effects of repeated seismic activity including densification and soil fabric changes that occur after cyclic loading phases. With these factors in mind, constant-volume cyclic direct simple shear tests were performed on a reconstituted Fraser River silt specimen that was normally consolidated initially to a vertical effective stress of 100 kPa. Tests with consecutive repeated cyclic loading phases were performed with increasing cyclic stress ratios. The cyclic shear response, including accumulation of shear strain and development of pore water pressure, from eight repeated cyclic shear loadings phases are presented herein.

1 INTRODUCTION

Recurrences of liquefaction at same sites during successive earthquakes have been reported in Japan (Kuribayashi & Tatsuoka, 1975; Wakamatsu, 2012; Yasuda & Tohno, 1988), Greece (Papathanassiou et al. 2016), United States of America (Sims & Garvin, 1995; Youd, 1984) and New Zealand (Kiyota et al. 2012; Orense et al. 2011; Quigley et al. 2013; Villemure et al. 2012).

Wakamatsu (2012) investigated 90 sites where repeated liquefaction was observed during the Great East Japan Earthquake in 2011and reported that the extent and severity of re-liquefaction effects observed for this earthquake are greater than those experienced at these sites during the previous liquefaction occurrences; the observations are in accord with the expectations since the intensity of the 2011 earthquake is greater than those from the previous shakings. The soil stratigraphy at most of the repeatedly liquefied locations comprised loose fine to medium sand within the upper 5 m depth zone with the groundwater levels within about 3 m from the ground surface. Youd (1984) postulated that seismic induced shear deformations can cause granular soils in shear zones to dilate and become further loose, in turn becoming more susceptible to liquefaction than before.

Investigating the effects of strain history for the liquefaction of sand through a laboratory experimental study, Finn et al. (1970) reported that if the cyclic shear strains exceed a threshold value, it would further weaken the cyclic shear resistance of test specimens against future cyclic loading; on the other hand, if the cyclic shear strains were lesser than that threshold value, it would result in a better interlocked particle structure (which would eliminate minor local instabilities) thereby causing an increase in cyclic shear resistance. Finn et al. (1970) further emphasized that cyclic shear resistance obtained through laboratory experimental tests on reconstituted sand specimens cannot be uniquely defined as a function of confining stress, void ratio, and peak cyclic shear stress alone, when the sand deposits in the field have undergone previous cyclic shearing.

Although sands have been widely investigated for recurrent liquefaction as per above, both field observation and studies focusing on recurrent liquefaction of silty sand and silty soil has been very limited. The Canterbury earthquake sequence in 2010-2011 induced wide spread liquefaction across the Christchurch urban area; Orense et al. (2011) and Villemure et al. (2012) have reported many examples of clear manifestations of recurrent liquefaction, and the intensity of effort required for sand-silt ejecta removal during the post-earthquake clearing process. Quigley et al. (2013) documented a unique example of such recurrent liquefaction of sand and silty soils with photographic evidence for a same location over six earthquakes from September 2010 to December 2011. From the evidence of those photos taken at the same location within three hours of the occurrence of each subsequent earthquake, it can be seen that the location, alignment, and the pattern of the cracks and fissures that served pathways for water, sand-silt ejecta during the initial liquefaction event were very similar to those observed during the initial and subsequent events of liquefaction.

Following liquefaction, soils would dissipate cyclic excess pore water pressures and re-consolidate, essentially resulting in post-seismic soil densification. The time-rate of consolidation in sands is relatively quicker than that for fine-grained soils, leaving moderately dense sand for the next event. However, fine-grained soils not only take time for the post-seismic re-consolidation, but also will likely experience significant changes in their particle fabric due to previous cyclic shear deformations. Therefore, repeated cyclic loading tests can serve to provide insight with respect to the effects of repeated seismic activity including densification and soil fabric changes. The current available literature and laboratory experimental studies on repeated cyclic loading on silts (Price et al. 2017) are very limited.

With these factors in mind, this paper presents and discusses the results of repeated constant-volume cyclic direct simple shear tests that were performed on reconstituted Fraser River silt. The main intent is to investigate the effects of previous cyclic shear loading phases on subsequent cyclic loadings. For the chosen silt, a comparison of cyclic shear loading responses observed from repeated cyclic loading on reconstituted specimens versus relatively undisturbed specimens are discussed.

2 EXPERIMENTAL ASPECTS

2.1 *Material tested*

Fraser River silt (excavated from the south bank of the Fraser River in an area east of the Port Mann Bridge in British Columbia) was used in this study. In preparing the soil samples for testing, Fraser River silt was oven dried and then sieved to remove the fine sand potion (coarser than 75 μm). Fraser River silt used in the repeated cyclic shear tests was non-plastic with a mean particle diameter of about 18 μm and a specific gravity of 2.72.

2.2 *Specimen preparation*

The reconstituted specimens were prepared using the slurry deposition method as described below. Initially, the soil was oven dried, and any clumps of dry soil were broken down using a pestle. A representative 125-g portion of dried soil was selected to prepare a given specimen and transferred into a 300 ml beaker. At this point, de-aired water was added to the soil while mixing until a homogeneous slurry was formed. The slurry was kept under vacuum for 24 hours for de-airing purposes. The sample was stirred, re-mixed, and shaken occasionally while it was under vacuum, in order to minimize the entrapped air bubbles inside the slurry. The sample was then allowed to consolidate under its own weight; at this point, the thin-clear excess water film formed at the top of the slurry was carefully siphoned out by applying suction. The remaining material was stirred once again, thus preparing a slurry mix that is ready to be gently placed in the specimen cavity surrounded by the wire-reinforced membrane. Significant care was exercised during specimen placement to minimize the formation of entrapped air in the reconstituted specimen.

The Direct Simple Shear (DSS) test device at the University of British Columbia (UBC), Canada was used for the testing work. The device accommodates a specimen with a diameter of about 70 mm and a height of about 20 mm placed in a wire-reinforced rubber membrane. The specimen is laterally confined by a wire-reinforced rubber membrane, and it enforces an essentially zero overall lateral strain during consolidation and shear deformation. Therefore, a constant-volume condition can be enforced by restraining the top and bottom loading platens of the specimen against vertical movement (i.e., by imposing a height constraint). It has been shown that the decrease (or increase) of vertical stress in a constant-volume DSS test is essentially equal to the increase (or decrease) of excess pore water pressure in an undrained DSS test where the near constant-volume condition is maintained by not allowing the mass of pore water to change (Dyvik et al. 1987). Therefore, in this test series, change of vertical stress during constant-volume shearing is interpreted as equivalent to change in excess pore-water pressure due to shear loading.

2.3 *Repeated constant-volume cyclic direct simple shear loading*

A given test specimen was initially consolidated to vertical effective consolidation stress (σ'_{vc}), of 100 kPa and then subjected to constant-volume, symmetrical, sinusoidal cyclic shear (τ_{cyc}) loading applied at a frequency of 0.1 Hz. The value of τ_{cyc} was selected to impose the desired constant cyclic stress ratio [$CSR = \tau_{cyc}/\sigma'_{vc}$] amplitude on the specimen. As an 'index' for assessing and comparing the cyclic shear strength, the attainment of 3.75 % single-amplitude horizontal shear strain (γ) in a DSS specimen was considered as a criterion for unacceptable performance, thus as a basis to terminate the cyclic shear loading test phase. Then, in preparation for the next cyclic shear loading with the desired CSR, the specimen was reconsolidated to 100 kPa. (Note: At the end of the final loading cycle during a given cyclic shear loading phase, the specimens invariably would possess residual shear strains; as such, the specimens were manually repositioned to zero shear strain level carefully and slowly, prior to reconsolidating to 100 kPa).

3 REPEATED CYCLIC LOADING RESPONSE

A reconstituted silt specimen prepared as per above was subjected to eight cyclic shearing stages, where the specimen was consolidated to 100 kPa prior to cyclic shearing in each shearing stage. The variations of the vertical effective stress and vertical strain of the test specimen with time for eight consolidation stages and subsequent cyclic shear loading are shown in Figure 1.

The specimen prepared by slurry deposition was consolidated to 100 kPa in four loading increments where it developed vertical strain of 14.5 % at the end of consolidation phase that lasted about three hours. In the following constant volume cyclic loading phase, it can be seen that the vertical effective stress would reduce due to the excess cyclic pore water pressure generation and that the vertical strain would remain constant meting the constant-volume condition. Vertical strain gained during each reconsolidation phase reduces with each successive reconsolidation phase. It can be also seen that variations of vertical effective stress during a loading cycle at later cyclic shearing stages are greater than those in earlier stages of cyclic shearing. Test parameters and summary of the results for these eight shearing stages of the reconstituted specimen are presented in Table 1.

Test ID intends to infer the details of specimen, shearing phase, void ratio and the cyclic shear stress of the test, for example, RS5-55-20 indicates Reconstituted Specimen at fifth shearing stage with a post-consolidation void ratio prior to the application of shearing (e_c) of 0.55 and cyclic stress ratio (CSR) of 0.20. With increasing number of cyclic shear stages that were followed by reconsolidation, it can be seen that the value of e_c would decrease systematically. After the seventh stage of cyclic shearing, the value of e_c equals to 0.5; clearly, this would not be achievable by simply consolidating a specimen to σ'_{vc} of 100 kPa.

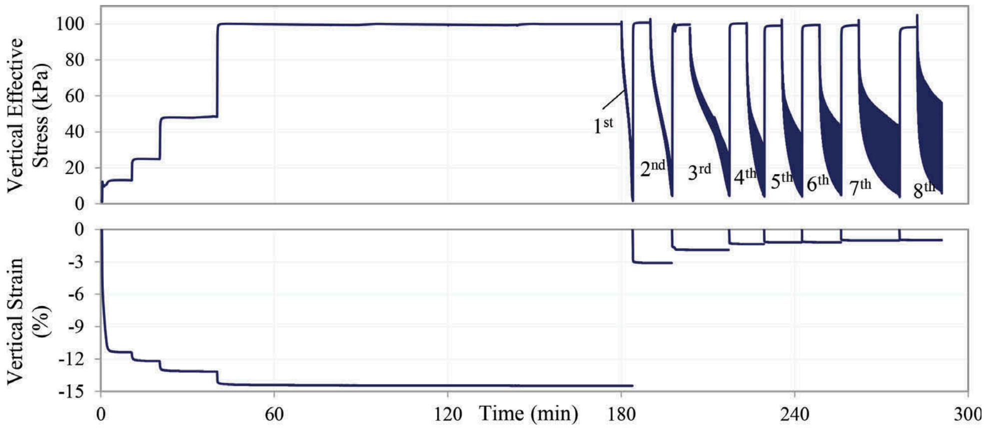

Figure 1. Vertical effective stress and vertical strain during 8 stages of repeated cyclic direct simple shear loading and reconsolidation for reconstituted silt

Table 1. Test parameters and summary of test results

Test ID	Shearing Stage	e_i	σ'_{vc}	e_c	CSR	$N_{cyc\ [\gamma=3.75\ \%]}$	$R_{u\text{-}max}$ %	γ_{max} %
RS1-68-11	1	0.96	100	0.68	0.11	21	0.92	7.01
RS2-63-11	2	0.68	100	0.63	0.11	44	0.93	4.03
RS3-59-14	3	0.63	100	0.59	0.14	80	0.93	4.07
RS4-57-17	4	0.59	100	0.57	0.17	34	0.93	3.94
RS5-55-20	5	0.57	100	0.55	0.20	38	0.94	3.83
RS6-54-23	6	0.55	100	0.54	0.23	44	0.94	3.89
RS7-52-23	7	0.54	100	0.52	0.23	84	0.94	3.81
RS8-50-29	8	0.52	100	0.50	0.29	51	0.93	3.81

e_i = Initial void ratio prior to consolidation CSR = Cyclic Stress Ratio
σ'_{vc} = Vertical effective consolidation stress prior to the application of shearing
e_c = Post-consolidation void ratio prior to the application of shearing
$N_{cyc\ [\gamma=3.75\ \%]}$ = Number of uniform loading cycles to reach single amplitude shear strain of 3.75%
$r_{u\text{-}max}$ = Maximum pore water pressure ratio during the cyclic shear loading phase
γ_{max} = Maximum shear strain during the cyclic shear loading phase

3.1 *Stress-strain and stress-path responses*

Some selected shear loading stages listed in Table 1 are presented in terms of stress-strain and stress-path responses in Figure 2. The specimen was sheared with increasing CSR in successive shearing stages, apart from the shearing stages 1 & 2, and 6 & 7. In these stage couples, the effect of decreasing void ratio by post-cyclic reconsolidation were studied with the magnitudes of CSR unchanged between the two phases.

From the stress-path response plots, general contractive tendency in behavior during the initial loading cycles, except for the first quarter cycle, can be seen. This is followed by dilative and contractive tendencies during loading and unloading potions of cyclic shear stress, respectively at later loading cycles. Further, it can be seen that the dilative tendency during loading phase and contractive tendency during unloading phase become increasingly intensified with increasing number of shearing stage with higher CSR. It can be seen that these changes observed in the shear loading characteristics from the reconstituted silt (as shown in Figure 2) is similar to the typical changes observed in shear loading response of sand when transitioning from low to high relative density conditions. At later repeated cyclic loading stages (i.e., in 6 & 7 shown in Figure 2), it begins to show dilative tendency in response even in the third quarter of the first loading cycle; when compared to that of initial or earlier repeated cyclic loading stages (i.e., in 1 to 4) where such responses are not visible.

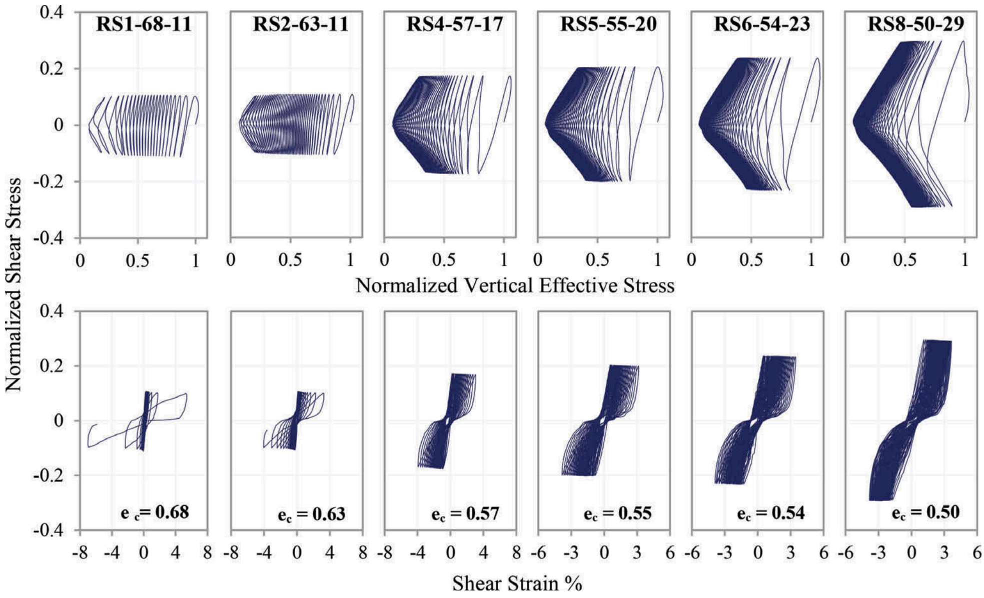

Figure 2. Stress-strain and stress-path responses of reconstituted specimens during repeated cyclic shear loading stages in constant-volume cyclic DSS tests

The stress-strain and stress-path responses observed during the shearing stages 1 & 2 and 6 & 7 (with a CSR of 0.23) are presented in Figure 3; herein, only the first and last two loading cycles for selected shearing stages are presented for the purpose of clarity. During the shearing stages 1 and 2, where the specimen underwent cyclic loading with identical values CSR of 0.11, the specimen survived 44 loading cycles before reaching a shear strain of 3.75 % in comparison to that of 21 loading cycles corresponding to the first shearing stage. The reduction of void ratio to 0.63 in the shearing stage 2 from a value of 0.68 in shearing stage 1 due to post-cyclic reconsolidation seems to be the reason for the observed greater cyclic shear resistance in stage 2 compared to stage 1. Similar increase in cyclic shear resistance can be identified in shearing stage 7 with respect to that in shearing stage 6, where reduction of void ratio from 0.54 to 0.52 and increase of $N_{cyc\ [\gamma\ =\ 3.75\ \%]}$ from 44 to 84 were shown for CSR of 0.23.

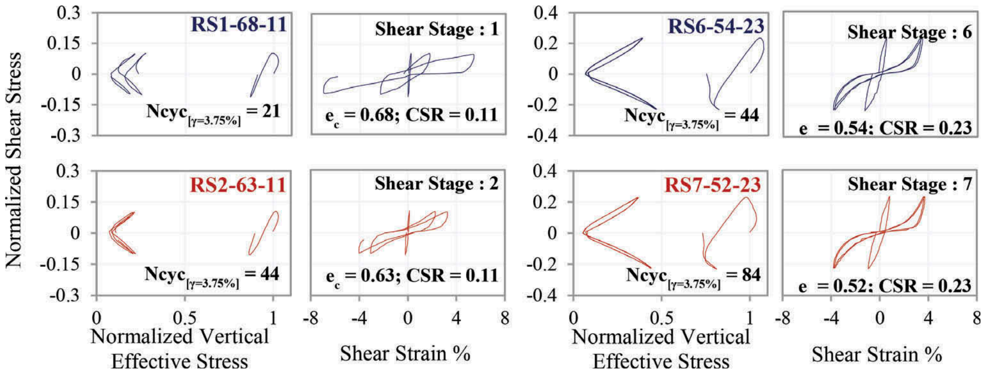

Figure 3. Stress-strain and stress-path responses of the first and the last two loading cycles for shearing stage 1-2 and 6-7 during repeated cyclic shear loading stages in constant-volume cyclic DSS tests

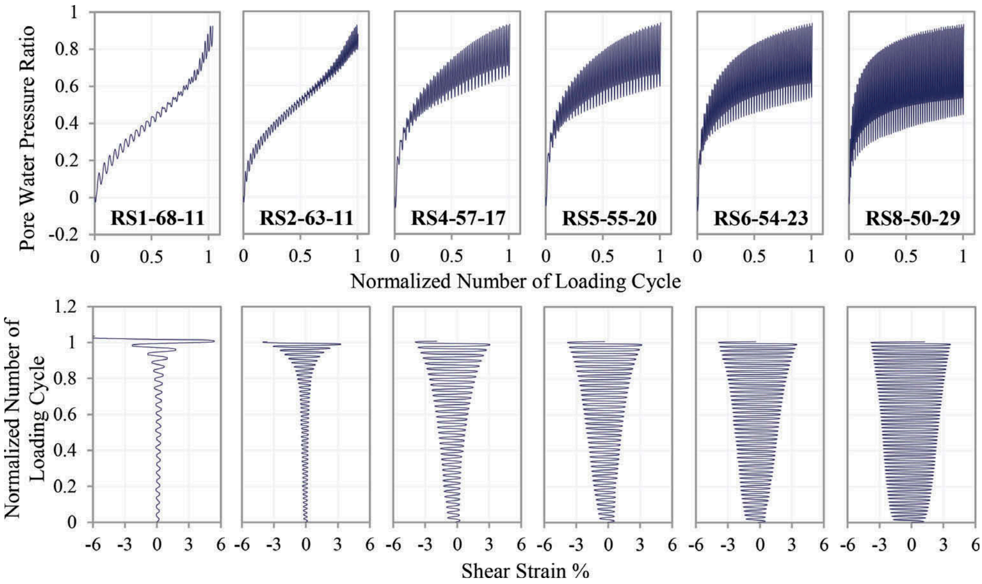

Figure 4. Accumulation of strain and generation of reconstituted specimens during repeated cyclic shear loading stages in constant-volume cyclic DSS tests

3.2 *Shear strain and pore water pressure responses*

Figure 4 presents the strain accumulation and pore water pressure generation during some selected shearing stages. As seen from Table 1, $N_{cyc\ [\gamma\ =\ 3.75\ \%]}$ ranges from 21 to 84 for different shearing stages which comprise different CSRs; the number of loading cycles have been normalized by $N_{cyc\ [\gamma\ =\ 3.75\ \%]}$ for the ease of comparison.

The excess pore water pressure generation during later shearing stages shown in Figure 4 indicates that the initial rates of rise in pore-water pressures are greater than those for earlier stages. Further, variation of the pore-water pressure during later loading cycles in higher shear stages are significantly greater than those for the shearing stage 1 and 2, this is also shown in the greater dilation tendencies in stress-path plots for higher shearing stages in Figure 2. It should be noted that the observed greater dilative tendencies with higher CSRs at later shearing stages occurred without the expenses of significant shear strain developments, especially at the loading cycles closer to $N_{cyc\ [\gamma\ =\ 3.75\ \%]}$ in comparison with those for shearing stage 1 and 2. For example, amount of strain accumulation over the successive last two loading cycles for the shearing stage 1 and 2 (refer Figure 3) are significantly higher than those for the shearing stage 6 and 7.

Once a specimen undergoes cyclic shearing, soil particles rearrange into a new structure that may depend on the amount of shear strain attained and excess pore water pressure developed during cyclic shearing. It can be postulated that the shear response observed during repeated cyclic loading herein is a reflection of the competing factors of reduction of void ratio (contributing for increase in cyclic shear resistance) and soil fabric induced from pre-shearing (possibly weakening the cyclic shear resistance). Thus, reduction of void ratio during the post cyclic reconsolidation phase may be identified as the main reason for the observed enhancement in cyclic shear resistance in both of the cases of shearing stage 1 & 2 and 6 & 7.

3.3 *Comparison of repeated cyclic loading response of reconstituted specimens and relatively undisturbed specimens*

Sanin (2005) performed cyclic shear tests for two repeated shearing stages on relatively undisturbed Fraser River silt specimens and reported that the $N_{cyc\ [\gamma\ =\ 3.75\ \%]}$ for second cyclic shearing stage was consistently less than those observed during the first cyclic shearing stage. Sanin

(2005) emphasized that the observed decrease in cyclic shear resistance in the repeated cyclic shearing stage may be due to the destructuration of soil fabric of relatively undisturbed specimen as a result of first shearing and that effect seemed to have overshadowed the any possible gain in cyclic shear resistance due to reduction of void ratio during post cyclic reconsolidation.

Similar type of conclusions have been reported by Sriskandakumar (2004) from the repeated cyclic shear loading response of water pluviated Fraser River sand specimens. Sriskandakumar (2004) indicated that if pre-shearing induces large shear strains, soil fabric weaken and the sand specimen undergoes liquefaction in the successive cyclic loading phases; whereas, small strains (shear strains do not exceeding 3.75%) experienced in the initial cyclic shearing phase appears to improve the cyclic shear resistance against liquefaction in the subsequent cyclic loading phase.

The results shown here indicate that the cyclic resistance of the reconstituted Fraser River silt specimen seems to be in an increasing trend with each repeated loading stage. Accordingly, it appears that the reduction of void ratio during each post-cyclic reconsolidation stage has effectively contributed to the observed increase in cyclic shear resistance, surpassing any influences due the change of soil fabric caused by cyclic shearing.

4 SUMMARY AND CONCLUSIONS

Constant-volume repeated cyclic DSS tests were conducted on a slurry-deposited reconstituted Fraser River specimen. Stress-strain, stress-path, strain and pore water pressure development were observed for eight repeated cyclic shear loading stages. The following observations and conclusions were noted in particular:

- The specimens became increasingly denser (void ratio decreases) during the post-cyclic reconsolidation related to each cyclic shearing stage; this behavior in turn, leads to increased dilative tendency during subsequent constant-volume cyclic DSS loading.
- The increased dilatancy, especially at later repeated cyclic shear loading stages, resulted in smaller shear strain increments over consecutive loading cycles; however, the variation of pore water pressure during a given loading cycle was wide and significant.
- The cyclic shear resistance of reconstituted Fraser River silt was observed to increase with increasing repeated cyclic shear loading stages. This is in contrast to the repeated cyclic shear response observed for relatively undisturbed Fraser River silt specimens, which showed decreasing cyclic shear resistance in comparison to that of initial cyclic shear loading phase.
- The different response of reconstituted and relatively undisturbed specimens in terms of cyclic shear resistance for repeated loading phases indicate the importance of factors such as void ratio, soil fabric, stress history in governing the cyclic shear resistance of soils.

ACKNOWLEDGEMENTS

The experimental research work was conducted with the financial support provided by the Natural Sciences and Engineering Research Council of Canada (NSERC) Discovery Grant (Application ID 2017-03846). Technical assistance of Scott Jackson, Harald Schremp, and Bill Leung of the Department of Civil Engineering Workshop is deeply appreciated.

REFERENCES

Dyvik, R., Berre, T., Lacasse, S. & Raadim, B. 1987. Comparison of truly undrained and constant volume direct simple shear tests. *Géotechnique*, 37(1): 3–10.

Finn, W. D. L., Bransby, P. L. & Pickering, D. J. 1970. Effect of Strain History on Liquefaction of Sand. *Journal of the Soil Mechanics and Foundations Division, ASCE*, 96(SM6): 1917–1934.

Kiyota, T., Yamada, S. & Hosono, Y. 2012. Repeated liquefaction observed during the 2010-2011 Canterbury Earthquakes. *Bulletin of Earthquake Resistant Structure Research Center*, Institute of Industrial Science, University of Tokyo, 45, 115–121.

Kuribayashi, E. & Tatsuoka, F. 1975. Brief review of liquefaction during earthquakes in Japan. *Soils and Foundations, Japanese Society of Soil Mechanics and Foundation Engineering*, 15(4): 81–92.

Orense, R. P., Kiyota, T., Yamada, S., Cubrinovski, M., Hosono, Y., Okamura, M. & Yasuda, S. 2011. Comparison of liquefaction Features observed during the 2010 and 2011 Canterbury earthquakes. *Seismological Research Letters*, 82(6),905–918.

Papathanassiou, G., Ganas, A. & Valkaniotis, S. 2016. Recurrent liquefaction-induced failures triggered by 2014 Cephalonia, Greece earthquakes: Spatial distribution and quantitative analysis of liquefaction potential. *Engineering Geology*, 200, 18–30.

Price, A. B., DeJong, J. T. & Boulanger, R. W. 2017. Cyclic loading response of silt with multiple loading events. *Journal of Geotechnical and Geoenvironmental Engineering, ASCE*, 143(10), 04017080

Quigley, M. C., Bastin, S. & Bradley, B. A. 2013. Recurrent liquefaction in Christchurch, New Zealand, during the Canterbury earthquake sequence. *Geology*, 41(4): 419–422.

Sanin, M. V. 2005. *Cyclic Shear Loading Response of Fraser River Delta Silt*. M.ASc. Thesis, The University of British Columbia.

Sims, J. D. & Garvin, C. D. 1995. Recurrent liquefaction induced by the 1989 Loma Prieta earthquake and 1990 and 1991 aftershocks: Implications for paleoseismicity studies. *Bulletin of the Seismological Society of America*, 85(1),51–65.

Sriskandakumar, S. 2004. *Cyclic loading response of Fraser River sand for validation of numerical models simulating centrifuge tests*. M.ASc. Thesis, The University of British Columbia.

Villemure, M., Wilson, T. M., Bristow, D. & Gallagher, M. 2012. Liquefaction ejecta clean-up in Christchurch during the 2010-2011 earthquake sequence. In *2012 Annual Technical Conference, New Zealand Society for Earthquake Engineering* (Paper Number 131).

Wakamatsu, K. 2012. Recurrence of liquefaction at the same site induced by the 2011 Great East Japan Earthquake compared with previous earthquakes. In *Proceedings of the 15th World Conference on Earthquake Engineering*. Lisbon, Portugal.

Yasuda, S. & Tohno, I. 1988. Sites of reliquefaction caused by the 1983 Nihonkai-Chubu earthquake. *Soils and Foundations, Japanese Society of Soil Mechanics and Foundation Engineering*, 28(2): 61–72.

Youd, T. L. 1984. Recurrence of liquefaction at the same site. In *Proceedings of the 8th World Conference on Earthquake Engineering*. San Francisco, California.